Activation of Akt Predicts Poor Outcome in Neuroblastoma

Daniela Opel,[1] Christopher Poremba,[2] Thorsten Simon,[3] Klaus-Michael Debatin,[1] and Simone Fulda[1]

[1]University Children's Hospital, Ulm, Germany; [2]Institute of Pathology, Heinrich-Heine-University, Düsseldorf, Germany; and [3]Children's Hospital, Paediatric Oncology, University of Cologne, Cologne, Germany

Abstract

Whereas aberrant activation of the phosphatidylinositol 3′-kinase (PI3K)/Akt pathway, a key survival cascade, has previously been linked to poor prognosis in several human malignancies, its prognostic effect in neuroblastoma has not yet been explored. We therefore investigated the phosphorylation status of Akt, S6 ribosomal protein as target of mammalian target of rapamycin, and extracellular signal–regulated kinase (ERK) in 116 primary neuroblastoma samples by tissue microarray and its correlation with established prognostic markers and survival outcome. Here, we provide for the first time evidence that phosphorylation of Akt at serine 473 (S473) and/or threonine 308 (T308), S6 ribosomal protein, and ERK frequently occurs in primary neuroblastoma. Importantly, we identified Akt activation as a novel prognostic indicator of decreased event-free or overall survival in neuroblastoma, whereas phosphorylation of S6 ribosomal protein or ERK had no prognostic effect. In addition, Akt activation correlated with variables of aggressive disease, including *MYCN* amplification, 1p36 aberrations, advanced disease stage, age at diagnosis, and unfavorable histology. Monitoring Akt at T308 or both phosphorylation sites improved the prognostic significance of Akt activation in neuroblastoma specimens compared with S473 phosphorylation. Parallel experiments in neuroblastoma cell lines revealed that activation of Akt by insulin-like growth factor (IGF)-I significantly inhibited tumor necrosis factor–related apoptosis-inducing ligand– or chemotherapy-induced apoptosis in a PI3K-dependent manner because the PI3K inhibitor LY294002 completely reversed the IGF-I–mediated protection of neuroblastoma cells from apoptosis. By showing that activation of Akt correlates with poor prognosis in primary neuroblastoma *in vivo* and with apoptosis resistance *in vitro*, our findings indicate that Akt presents a clinically relevant target in neuroblastoma that warrants further investigation. [Cancer Res 2007;67(2):735–45]

Introduction

Neuroblastoma is the most common extracranial solid tumor in childhood and accounts for 7% to 10% of pediatric malignancies (1). Currently, even intensive, multimodality therapy has resulted in only modest improvement in the cure rate of the more aggressive neuroblastoma (2, 3). Neuroblastoma is a leading cause of morbidity and mortality in children (1). Because a better understanding of the tumor biology of neuroblastoma may lead to biologically based therapies that are more effective and less toxic, there has recently been much interest in identifying molecular pathways that are involved in progression of neuroblastoma (4).

The phosphatidylinositol 3′-kinase (PI3K) pathway, in particular, seems to be one of the most potent prosurvival signaling pathways (5). Deregulated signaling through the PI3K pathway is common in many types of human malignancies, including glioblastoma and breast, prostate, and lung cancers (5, 6). For example, activation of the PI3K/Akt pathway has recently been reported to correlate with increasing tumor grade, decreased apoptosis, and adverse clinical outcome in glioblastoma *in vivo* (7, 8). Aberrant activation of the PI3K/Akt pathway in cancers can be caused by genetic lesions [e.g., mutations of the tumor suppressor gene phosphatase and tensin homologue (*PTEN*)] or by tyrosine kinase receptors stimulated by growth factors [e.g., insulin-like growth factor (IGF), epidermal growth factor, or brain-derived neurotrophic factor (BDNF); refs. 5, 9–11]. Critical mediators of PI3K, including Akt and mammalian target of rapamycin (mTOR), are known to enhance cellular survival by stimulating cell proliferation, glucose metabolism, or angiogenesis and by actively suppressing apoptosis (5, 10). Akt is a serine/threonine kinase that is activated by a dual regulatory mechanism that requires both translocation to the plasma membrane and phosphorylation of two key amino acids (5). On growth factor stimulation, PI3K generates phosphatidylinositol 3,4-bisphosphate and phosphatidylinositol-3,4,5-triphosphate, which bind to the pleckstrin homology domains of Akt and 3′-phosphoinositide-dependent kinase-1 (PDK-1), promoting their translocation to the plasma membrane, where Akt becomes phosphorylated in the catalytic domain at threonine 308 (T308) by PDK-1 (5). In addition, Akt is phosphorylated in the regulatory domain at serine 473 (S473) through mechanisms not completely resolved (5). Phosphorylation of Akt at both T308 and S473 is required for full kinase activity (5).

Programmed cell death or apoptosis plays a pivotal role in the regulation of tissue homeostasis, which is maintained by a balance between proliferation and cell death (12–14). Accordingly, a reduction of the physiological rate of apoptosis may contribute to tumor formation and progression (15). In addition, apoptosis has been implicated to mediate therapy-induced cytotoxicity (e.g., following chemotherapy, γ-irradiation, or immunotherapy; ref. 13). Apoptosis pathways may be initiated through the extrinsic (death receptor) or intrinsic (mitochondrial) pathway, resulting in activation of effector caspases (13). Stimulation of death receptors of the tumor necrosis factor (TNF) receptor superfamily such as TNF-related apoptosis-inducing ligand (TRAIL) receptors results in activation of caspase-8, which initiates direct cleavage of downstream effector caspases (16). The mitochondrial pathway is, for example, engaged in response to cytotoxic drug treatment and

involves the release of apoptogenic factors, such as cytochrome *c* or second mitochondria-derived activator of caspase (Smac)/direct inhibitor of apoptosis– binding protein with low isoelectric point (DIABLO), from mitochondria into the cytosol, triggering caspase-3 activation as a result of formation of the apoptosome complex (17).

Despite growing interest in the PI3K/Akt pathway as cancer drug target in recent years (18, 19), the activation status and the potential clinical prognostic value of components of this pathway have not yet been explored in clinical specimens in neuroblastoma. Therefore, we investigated activation of the PI3K/Akt pathway and its correlation with established prognostic markers and survival outcome in a large cohort of neuroblastoma patients in the present study. Parallel experiments in neuroblastoma cell lines were designed to analyze the effect of elevated PI3K/Akt signaling on apoptosis sensitivity.

Materials and Methods

Tissue Microarray

Patients. A total of 116 patients of the Cooperative German Neuroblastoma Trials NB90, NB95, and NB97 were analyzed by tissue microarray. Briefly, representative tissue blocks were selected as donor blocks for the tissue microarray. Sections were cut from each donor block and stained with H&E. Using these slides, one morphologically representative region was chosen from each of the 116 neuroblastoma samples. One cylindrical core tissue specimen per tumor block (diameter, 2.0 mm) was punched from these regions and precisely arrayed into a new recipient paraffin block using a custom-built precision instrument (Beecher Instruments, Silver Spring, MD). Tumor samples were taken before chemotherapy. Characteristics of patients' tumors are summarized in Supplementary Table S1.

Immunohistochemistry. Three-micrometer sections were prepared from the tissue microarray and mounted onto silane-coated glass slides. Immunohistochemical analyses were done with rabbit anti–phospho-Akt (S473) monoclonal antibody (1:100; Cell Signaling, Beverly, MA), rabbit anti–phospho-Akt (T308) monoclonal antibody (1:100; Cell Signaling), rabbit anti–phospho-S6 ribosomal protein (S235/236) polyclonal antibody (1:400; Cell Signaling), and rabbit anti–phospho-extracellular signal–regulated kinase (ERK; T202/Y204) monoclonal antibody (E10; 1:400; Cell Signaling). Pretreatment for antigen retrieval was done with pressure cooker (10 mmol/L sodium citrate buffer pH 6.0, 10 min). After blockage of biotin and peroxidase, immunohistochemical staining was done on an automated immunostainer (i6000, Biogenex, San Ramon, CA) using the standard labeled streptavidin-biotin method (UltraTek Reagent Detection Kit, Scy Tek, Logan, UT) followed by 3,3′-diaminobenzidine enzymatic development. Sections were counterstained blue with hematoxylin. Omission of the primary antibody served as negative control. Immunohistochemical stainings were evaluated by a pathologist (C.P.), who was blinded to all clinical variables, semiquantitatively by percentage of stained tumor cells and staining intensity (low phosphorylation: intermediate or strong staining in <1% of tumor cells; high phosphorylation: intermediate or strong staining in >50% of tumor cells).

Analysis of *MYCN* amplification and chromosomal alterations. Determination of the *MYCN* status was assessed in neuroblastoma tumors by fluorescence *in situ* hybridization (FISH), PCR, or Southern blot analysis. According to the European Network for Quality Assurance in Higher Education guidelines (20), *MYCN* amplification was defined as a >4-fold increase of *MYCN* signal number in relation to the number of chromosomes 2. Chromosomal aberrations in 1p36 were investigated in neuroblastoma tumors using FISH or PCR.

Statistical analysis of tissue microarray. To compare variables of interest, χ^2 test or Fisher's exact test was used where appropriate. Survival curves were calculated according to Kaplan-Meier and compared with log-rank test. Event-free survival was calculated as the time from diagnosis to event, or last examination if the patient had no event. Recurrence, progression of disease, and death from disease were counted as events. Overall survival was calculated as the time from diagnosis to death, or last examination if the patient survived. Death resulting from therapy complications ($n = 6$) as well as development of secondary malignant disease ($n = 1$) was censored for event-free survival and overall survival analysis.

Cell Culture and Chemicals

Neuroblastoma cell lines were maintained in RPMI 1640 or DMEM (Life Technologies, Inc., Eggenstein, Germany), supplemented with 10% FCS (Biochrom, Berlin, Germany), 1 mmol/L glutamine (Biochrom), 1% penicillin/streptavidin (Biochrom), and 25 mmol/L HEPES (Biochrom) as previously described (21). Chemicals were purchased from Sigma (Deisenhofen, Germany) unless otherwise indicated, IGF-I or IGF-II from Biochrom, recombinant TRAIL from R&D Systems, Inc. (Wiesbaden, Germany), and doxorubicin, cisplatin, and the PI3K inhibitor LY294002 from Sigma.

Determination of Apoptosis

For determination of apoptosis, SH-EP or SH-SY5Y neuroblastoma cells ($0.5 \times 10^5/cm^2$ and $1 \times 10^5/cm^2$, respectively) were seeded in 24-well plates (Falcon, Heidelberg, Germany), allowed to settle for 24 h, washed once with PBS (Biochrom), pretreated or not with IGF-I or IGF-II for 4 h or with LY294002 for 1 h, and then treated with TRAIL, doxorubicin, or cisplatin in the presence or absence of IGF-I, IGF-II, or LY294002 in serum-free medium. Apoptosis was determined by fluorescence-activated cell sorting (FACS; FACScan, BD Biosciences, Heidelberg, Germany) analysis of DNA fragmentation of propidium iodide–stained nuclei as previously described (21). The percentage of specific apoptosis was calculated as follows: $100 \times$ [experimental apoptosis (%)] / [100% − spontaneous apoptosis in medium (%)].

Surface Staining

To analyze expression of IGF receptor, 5×10^5 nonfixed SH-EP and SH-SY5Y neuroblastoma cells were incubated with IGF-I receptor monoclonal antibody (Oncogene, Bad Soden, Germany) or antimouse immunoglobulin G (IgG)-1 control antibody (Dako, Hamburg, Germany) for 30 min at 4°C, washed once with PBS containing 1% FCS, incubated for 30 min at 4°C in the dark with secondary antimouse phycoerythrin-conjugated antibody (Dako), washed once with PBS containing 1% FCS, and then analyzed by flow cytometry.

Western Blot Analysis

Neuroblastoma cells seeded overnight in 10-cm plates or 75-cm² flasks were treated or not with IGF-I, IGF-II, or LY294002 in medium containing 0% FCS or 10% FCS for indicated time points. Cells were lysed for 15 min on ice in lysis buffer [30 mmol/L Tris-HCl (pH 7.5), 150 mmol/L NaCl, 1% Triton-X, 10% glycerol, 2 mmol/L DTT, 200 μmol/L phenylmethylsulfonyl fluoride, 1 mmol/L Na_3VO_4, 10 nmol/L okadaic acid, 1 mmol/L β-glycerophosphate, 1 mmol/L EDTA, 50 mmol/L sodium fluoride, and a mixture of proteinase inhibitors (Roche, Mannheim, Germany)], followed by high-speed centrifugation. Fifty micrograms of lysate were separated on a 10% SDS-PAGE and electroblotted onto a Hybond enhanced chemiluminescence nitrocellulose membrane (Amersham Pharmacia Biotech, Freiburg, Germany). Membranes were blocked for 1 h in PBS supplemented with 5% milk powder and 0.1% Tween 20. Membranes were stained overnight with primary antibody, followed by 1-h incubation with horseradish peroxidase–conjugated secondary antibody, and detection was done with enhanced chemiluminescence (Amersham Pharmacia).

The following antibodies were used: rabbit anti–phospho-Akt (S473) polyclonal antibody (1:1,000; Cell Signaling), rabbit anti–phospho-Akt (T308) monoclonal antibody (244F9; 1:1,000; Cell Signaling), mouse anti-Akt monoclonal antibody (1:500; BD Bioscience), rabbit anti–phospho-S6 ribosomal protein (S235/236) polyclonal antibody (1:1,000; Cell Signaling), rabbit anti–S6 ribosomal protein polyclonal antibody (1:1,000; Cell Signaling), mouse anti–phospho-ERK (T202/Y204) monoclonal antibody (E10; 1:2,000; Cell Signaling), or rabbit anti-ERK polyclonal antibody (1:10,000; Sigma). Horseradish peroxidase–conjugated goat anti-mouse

IgG or goat anti-rabbit IgG (1:5,000) was obtained from Santa Cruz Biotechnology (Santa Cruz, CA). Mouse anti–β-actin monoclonal antibody (1:5,000; Sigma) was used as loading control.

Results

Activation of the PI3K/Akt pathway in primary neuroblastoma samples. Whereas the PI3K/Akt pathway has elicited intense interest as drug target in several types of cancer (6–8), its activation status has not yet been explored in neuroblastoma *in vivo*. Therefore, we analyzed phosphorylation of Akt, a target of PI3K, and S6 ribosomal protein, a target of mTOR, as read-outs for activation of upstream and downstream components of the pathway by immunohistochemistry using a human tissue microarray composed of 116 primary neuroblastoma specimens. Because

full activation of Akt requires phosphorylation of two key amino acids in the regulatory (S473) and catalytic domains (T308; ref. 5), we monitored phosphorylation of both sites to allow a thorough analysis of Akt activation. We found that Akt was highly phosphorylated at S473 in 61.2% (71 of 116) and at T308 in 62.9% (73 of 116) of primary neuroblastoma (Fig. 1*A*). Of 116 tumors, 66 (56.9%) were positive for both phosphospecific Akt antibodies (Fig. 1*A* and *B*). Five of 116 (4.3%) of neuroblastoma specimens were positive for S473 phosphorylation but not T308 phosphorylation, whereas 7 of 116 (6%) were positive for T308 phosphorylation but not S473 phosphorylation (Fig. 1*B*). Thirty-eight of 116 (32.8%) tumors showed low phosphorylation of both sites (Fig. 1*B*). Strong phosphorylation of S6 ribosomal protein, a target of mTOR, occurred in 55.2% (64 of 116) of neuroblastoma samples
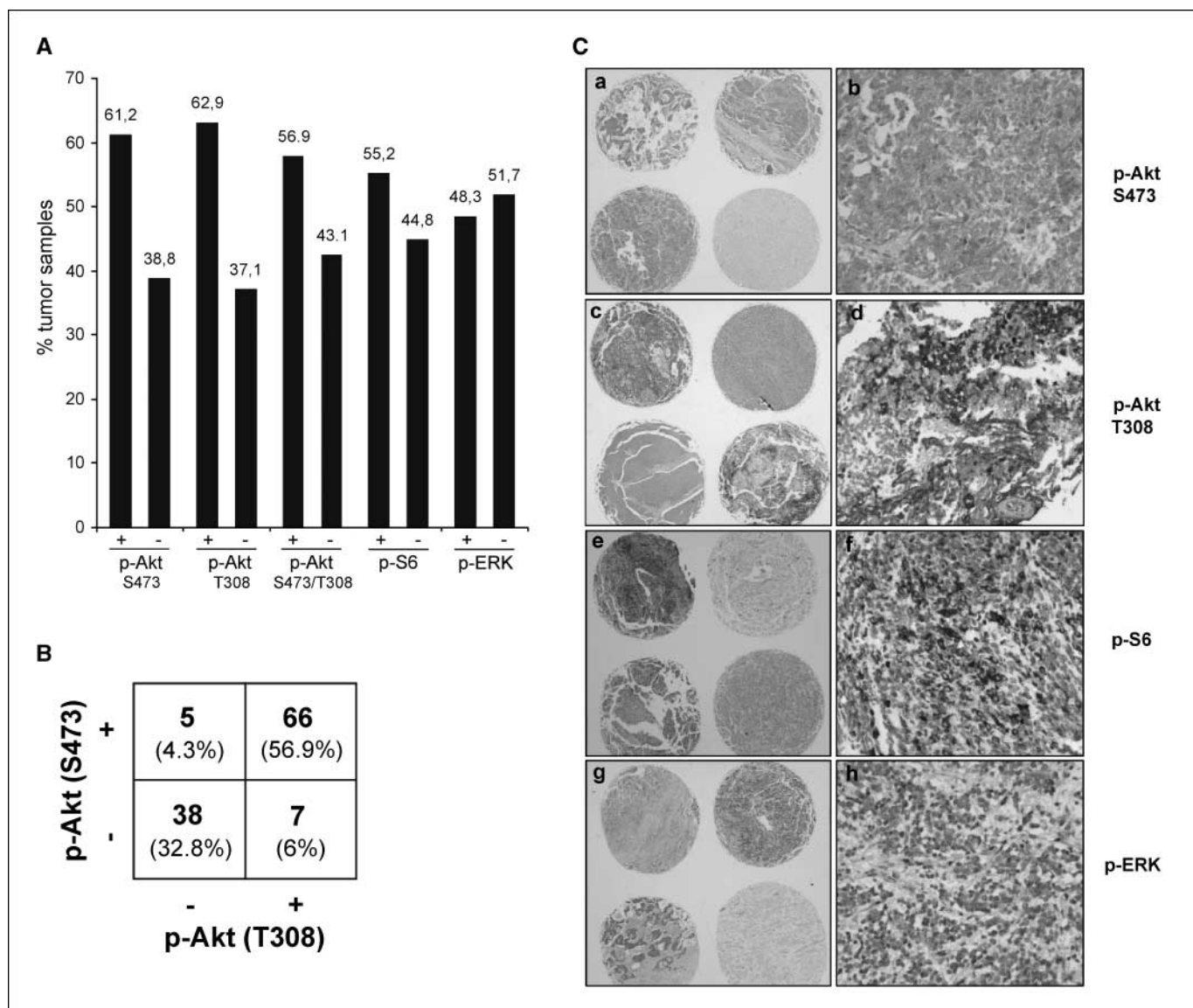

Figure 1. Activation of the PI3K/Akt pathway in primary neuroblastoma samples. Phosphorylation of Akt, S6 ribosomal protein, and ERK was analyzed in primary neuroblastoma samples by immunohistochemistry on a tissue microarray chip containing 116 neuroblastoma samples. *A,* percentage of tumor samples showing high (+) or low (−) phosphorylation of Akt at S473 (AktS473), at T308 (AktT308), at both S473 and T308 (AktS473/T308), S6 ribosomal protein, and ERK. *B,* number and percentage of neuroblastoma samples with low (−) or high (+) phosphorylation of Akt at S473 and/or T308. *C,* representative immunohistochemical stainings of phospho-AktS473 (*a* and *b*), phospho-AktT308 (*c* and *d*), phospho-S6 ribosomal protein (*e* and *f*), and phospho-ERK (*g* and *h*). Magnification, ×20 (*a, c, e,* and *g*), ×200 (*b, d, f,* and *h*).

Table 1. Correlation of the phosphorylation status of Akt, S6 ribosomal protein, or ERK and variables of aggressive disease in primary neuroblastoma

MYCN	Low p-AktS473	High p-AktS473	Low p-AktT308	High p-AktT308
(A) Phosphorylation status of Akt, S6, or ERK and *MYCN* amplification				
Nonamplified	40/41 (97.6%)	56/69 (81.2%)	40/40 (100%)	56/70 (80.0%)
Amplified	1/41 (2.4%)	13/69 (18.8%)	0/40 (0%)	14/70 (20.0%)
Fisher's		*P* = **0.016**		*P* = **0.002**
(B) Phosphorylation status of Akt, S6, or ERK and 1p36 aberrations				
No aberrations	19/19 (100%)	18/25 (72%)	20/20 (100%)	17/24 (70.8%)
Aberrations	0/19 (0%)	7/25 (28%)	0/20 (0%)	7/24 (29.2%)
Fisher's		*P* = **0.014**		*P* = **0.011**
(C) Phosphorylation status of Akt, S6, or ERK and disease stage				
Stage I–III	34/45 (75.6%)	42/71 (59.2%)	35/43 (81.4%)	41/73 (56.2%)
Stage IV	9/45 (20.0%)	25/71 (35.2%)	6/43 (14.0%)	28/73 (38.4%)
Stage IVS	2/45 (4.4%)	4/71 (5.6%)	2/43 (4.7%)	4/73 (5.5%)
χ^2 test		*P* = 0.184		*P* = **0.017**
(D) Phosphorylation status of Akt, S6, or ERK and age 12 mo at diagnosis				
Age <12 mo	14/45 (31.1%)	23/71 (32.4%)	14/43 (32.6%)	23/73 (31.5%)
Age >12 mo	31/45 (68.9%)	48/71 (67.6%)	29/43 (67.4%)	50/73 (68.5%)
Fisher's		*P* = 1.000		*P* = 1.000
(E) Phosphorylation status of Akt, S6, or ERK and age 18 mo at diagnosis				
Age <18 mo	30/45 (66.6%)	41/71 (57.7%)	31/43 (72.1%)	40/73 (54.8%)
Age >18 mo	15/45 (33.3%)	30/71 (42.3%)	12/43 (27.9%)	33/73 (45.2%)
Fisher's		*P* = 0.435		*P* = 0.077
(F) Phosphorylation status of Akt, S6, or ERK and age 24 mo at diagnosis				
Age <24 mo	33/45 (73.3%)	45/71 (63.4%)	34/43 (79.1%)	44/73 (60.3%)
Age >24 mo	12/45 (26.7%)	26/71 (36.6%)	9/43 (20.9%)	29/73 (39.7%)
Fisher's		*P* = 0.313		*P* = **0.042**
(G) Phosphorylation status of Akt, S6, or ERK and Shimada classification				
Favorable	34/42 (81.0%)	41/66 (62.1%)	35/40 (87.5%)	40/68 (58.8%)
Unfavorable	8/42 (19.0%)	25/66 (37.9%)	5/40 (12.5%)	28/68 (41.2%)
Fisher's		*P* = 0.053		*P* = **0.002**

NOTE: Phosphorylation of Akt at S473 (AktS473) or at T308 (AktT308), S6 ribosomal protein, and ERK was analyzed by immunohistochemistry on a tissue microarray and correlated with *MYCN* amplification (*A*), 1p36 aberrations (*B*), disease stage (*C*), age at diagnosis (*D–F*), or Shimada classification (*F*) using χ^2 test or Fisher's exact test (Fisher's) as indicated. Statistically significant correlations are indicated in bold; AktS/T, Akt phosphorylation at S473 and T308; mo, months.

(Fig. 1*A*). Because interactions between the PI3K/Akt and the Raf/mitogen-activated protein kinase kinase (MEK)/ERK pathways have been described (22–24), we also assessed phosphorylation of ERK, a direct target of MEK. High phosphorylation of ERK was detected in 48.3% (56 of 116) of primary neuroblastoma specimens (Fig. 1*A*). Representative immunohistochemical stainings of phospho-Akt (S473 and T308), phospho-S6 ribosomal protein, and phospho-ERK are shown in Fig. 1*C*.

We also investigated whether there is a correlation among the phosphorylation status of Akt, S6 ribosomal protein, and ERK. We found a correlation of phosphorylation of Akt at S473, T308, or both S473 and T308 and S6 ribosomal protein (*P* = 0.004, *P* = 0.004, and *P* = 0.001, respectively; χ^2 test), phosphorylation of Akt at S473 and T308 (*P* = <0.001, χ^2 test), phosphorylation of S6 ribosomal protein and ERK (*P* = <0.001, χ^2 test), as well as phosphorylation of Akt at S473 or both S473 and T308 and ERK (*P* = 0.036 and *P* = 0.015, respectively; χ^2 test), whereas there was no correlation of phosphorylation of Akt at T308 and ERK (*P* = 0.18, χ^2 test). These results may reflect that Akt and S6 ribosomal protein are upstream and downstream components of the PI3K/Akt/mTOR pathway and that cross-talks between ERK and the PI3K/Akt/mTOR pathway

may exist, which can both be activated by ligation of growth factor receptors (9). Together, this set of experiments shows that phosphorylation of Akt at S473 and/or T308 as well as phosphorylation of S6 ribosomal protein and ERK occurs in a large proportion of neuroblastoma specimens. This indicates that the PI3K/Akt and Raf/MEK/ERK pathways are frequently activated in neuroblastoma *in vivo*.

Activation of the PI3K/Akt pathway and advanced disease. We next asked whether or not activation of the PI3K/Akt pathway was associated with variables of advanced disease in neuroblastoma. To address this question, we correlated phosphorylation of Akt, S6 ribosomal protein, or ERK with various established variables used for prognostic stratification of neuroblastoma, including *MYCN* amplification, 1p36 aberrations, stage of disease, age at diagnosis, and tumor histology (1). Interestingly, we found that high phosphorylation of Akt at S473, T308, or both phosphorylation sites significantly correlated with *MYCN* amplification or 1p36 aberrations (Table 1*A* and *B*). The level of significance increased for correlation of Akt phosphorylation and *MYCN* amplification, when phosphorylation at T308 or at both sites was assessed compared with phosphorylation at S473 (Table 1*A*). In addition, there was a

Table 1. Correlation of the phosphorylation status of Akt, S6 ribosomal protein, or ERK and variables of aggressive disease in primary neuroblastoma (Cont'd)

Low p-AktS/T	High p-AktS/T	Low p-S6	High p-S6	Low p-ERK	High p-ERK
45/45 (100%)	51/65 (78.5%)	42/49 (85.7%)	54/61 (8.5%)	50/57 (87.7%)	46/53 (86.8%)
0/45 (0%)	14/65 (21.5%)	7/49 (14.3%)	7/61 (11.5%)	7/57 (12.3%)	7/53 (13.2%)
	P = **0.001**		*P* = 0.776		*P* = 1.000
22/22 (100%)	15/22 (68.2%)	15/18 (83.3%)	22/26 (84.6%)	22/26 (84.6%)	15/18 (83.3%)
0/22 (0%)	7/22 (31.8%)	3/18 (16.7%)	4/26 (15.4%)	4/26 (15.4%)	3/18 (16.6%)
P = **0.011**	*P* = **0.009**		*P* = 1.000		*P* = 1.000
39/50 (78.0%)	37/66 (56.1%)	37/52 (71.2%)	39/64 (60.9%)	43/60 (71.6%)	33/56 (58.9%)
9/50 (18.0%)	25/66 (37.9%)	14/52 (26.9%)	20/64 (31.3%)	14/60 (23.3%)	20/56 (35.7%)
4/73 (5.5%)	4/66 (6.1%)	1/52 (1.9%)	5/64 (7.8%)	3/60 (5%)	3/56 (5.4%)
	P = **0.046**		*P* = 0.277		*P* = 0.326
16/50 (32.0%)	21/66 (31.8%)	21/52 (40.4%)	16/64 (25.0%)	21/60 (35.0%)	16/56 (28.6%)
34/50 (68.0%)	45/66 (68.2%)	31/52 (59.6%)	48/64 (75.0%)	39/60 (65.0%)	40/56 (71.4%)
	P = 1.000		*P* = 0.109		*P* = 0.551
35/50 (70.0%)	36/66 (54.5%)	35/52 (67.3%)	36/64 (56.3%)	37/60 (61.6%)	34/56 (60.7%)
15/50 (30.0%)	30/66 (46.5%)	17/52 (32.7%)	28/64 (43.7%)	23/60 (38.4%)	22/56 (39.3%)
	P = 0.057		*P* = 0.254		*P* = 1.000
38/50 (76.0%)	40/66 (60.6%)	36/52 (69.2%)	42/64 (65.6%)	40/60 (66.7%)	38/56 (67.9%)
12/50 (24.0%)	26/66 (39.4%)	16/52 (30.8%)	22/64 (34.4%)	20/60 (33.3%)	18/56 (32.1%)
	P = **0.048**		*P* = 0.696		*P* = 1.000
12/50 (24.0%)	36/61 (59.0%)	38/50 (76.0%)	37/58 (63.8%)	40/57 (70.2%)	35/51 (68.6%)
8/47 (17.0%)	25/61 (41.0%)	12/50 (24.0%)	21/58 (36.2%)	17/57 (29.8%)	16/51 (31.4%)
	P = **0.006**		*P* = 0.211		*P* = 1.000

stronger correlation between phosphorylation of both Akt sites and 1p36 aberrations compared with either phosphorylation site alone (Table 1*B*). Moreover, Akt phosphorylation at T308 or at both sites, but not at S473, correlated with stage IV disease, age >24 months at diagnosis, and unfavorable histology according to Shimada classification (Table 1*C*, *F*, and *G*). These findings indicate that monitoring Akt at T308 or both phosphorylation sites improves the assessment of Akt activation. In contrast, no significant association was observed between high phosphorylation of S6 ribosomal protein or ERK and any of the variables tested (Table 1). Thus, Akt activation, but not phosphorylation of S6 ribosomal protein as read-out of mTOR activity or ERK, correlates with variables of advanced disease in neuroblastoma.

Activation of the PI3K/Akt pathway and survival. We then went on to evaluate the prognostic value of the PI3K/Akt pathway in neuroblastoma. All patients were treated according to the protocols of the Cooperative German Neuroblastoma Trials (NB90, NB95, and NB97). The cumulative event-free survival curves of neuroblastoma patients with high or low phosphorylation of Akt, S6 ribosomal protein, or ERK in tumor samples are shown in Fig. 2, and 3-year event-free and overall survival of patients are summarized in Table 2. Importantly, we found that high phosphorylation of Akt at S473, T308, or both sites significantly correlated with reduced event-free and overall survival in Kaplan-Meier analysis for the group of 116 neuroblastoma patients (Fig. 2*A*; Table 2). Monitoring Akt at T308 or both phosphorylation sites

improved the predictive prognostic value of Akt activation compared with Akt phosphorylation at S473. In contrast, high phosphorylation of S6 ribosomal protein or ERK was not associated with event-free or overall survival of neuroblastoma patients (Fig. 2*B* and *C*; Table 2). These findings show that high phosphorylation of Akt, but not of S6 ribosomal protein as read-out of mTOR activity or ERK, predicts event-free and overall survival of neuroblastoma patients.

Activation of the PI3K/Akt pathway in neuroblastoma cell lines. Next, we asked whether or not the PI3K/Akt pathway was constitutively activated in neuroblastoma cell lines. To address this question, we cultured a panel of human neuroblastoma cell lines for 24 h in the absence of serum (0% FCS) or, for comparison, in the presence of serum (10% FCS). As shown in Fig. 3, we found no constitutive phosphorylation of Akt at S473 in neuroblastoma cell lines after complete serum deprivation for 24 h. Some phosphorylation of Akt at S473 was detected in SK-N-SH, SK-N-BE, SH-EP, SH-SY5Y, and IMR32 neuroblastoma cell lines when cells were cultured in medium containing 10% FCS (Fig. 3). Phosphorylation of S6 ribosomal protein, a downstream target of mTOR, was not detectable in most neuroblastoma cell lines and low in SH-EP neuroblastoma cells under serum deprivation (Fig. 3). Variable phosphorylation of S6 ribosomal protein was found in neuroblastoma cell lines cultured in medium containing 10% FCS (Fig. 3). By comparison, ERK was phosphorylated in SK-N-SH, SK-N-AS, SH-EP, and SH-SY5Y neuroblastoma cells and, to some extent, also

in SK-N-BE, Kelly, and IMR32 neuroblastoma cells even in the absence of serum (Fig. 3). U87MG glioblastoma cells were used as a positive control for constitutive phosphorylation of Akt, S6 ribosomal protein, and ERK even under serum deprivation (Fig. 3).

Growth factors (e.g., IGF-I) are known to stimulate Akt (10). Because the IGF system has been implicated to play an important role in neuroblastoma biology (11), we next used IGF-I to activate Akt. Stimulation of neuroblastoma cells with IGF-I resulted in

strong phosphorylation of AktS473 and S6 ribosomal protein (Fig. 3). By comparison, phosphorylation of ERK was enhanced by IGF-I in some cell lines (i.e., SK-N-BE, SK-N-AS, Kelly, and IMR32 cells; Fig. 3). Monitoring Akt phosphorylation at T308 yielded similar results compared with phosphorylation of Akt at S473 in neuroblastoma cell lines (Supplementary Fig. S1). We therefore assessed Akt phosphorylation at S473 to determine Akt activation in SH-EP and SH-SY5Y neuroblastoma cells in subsequent
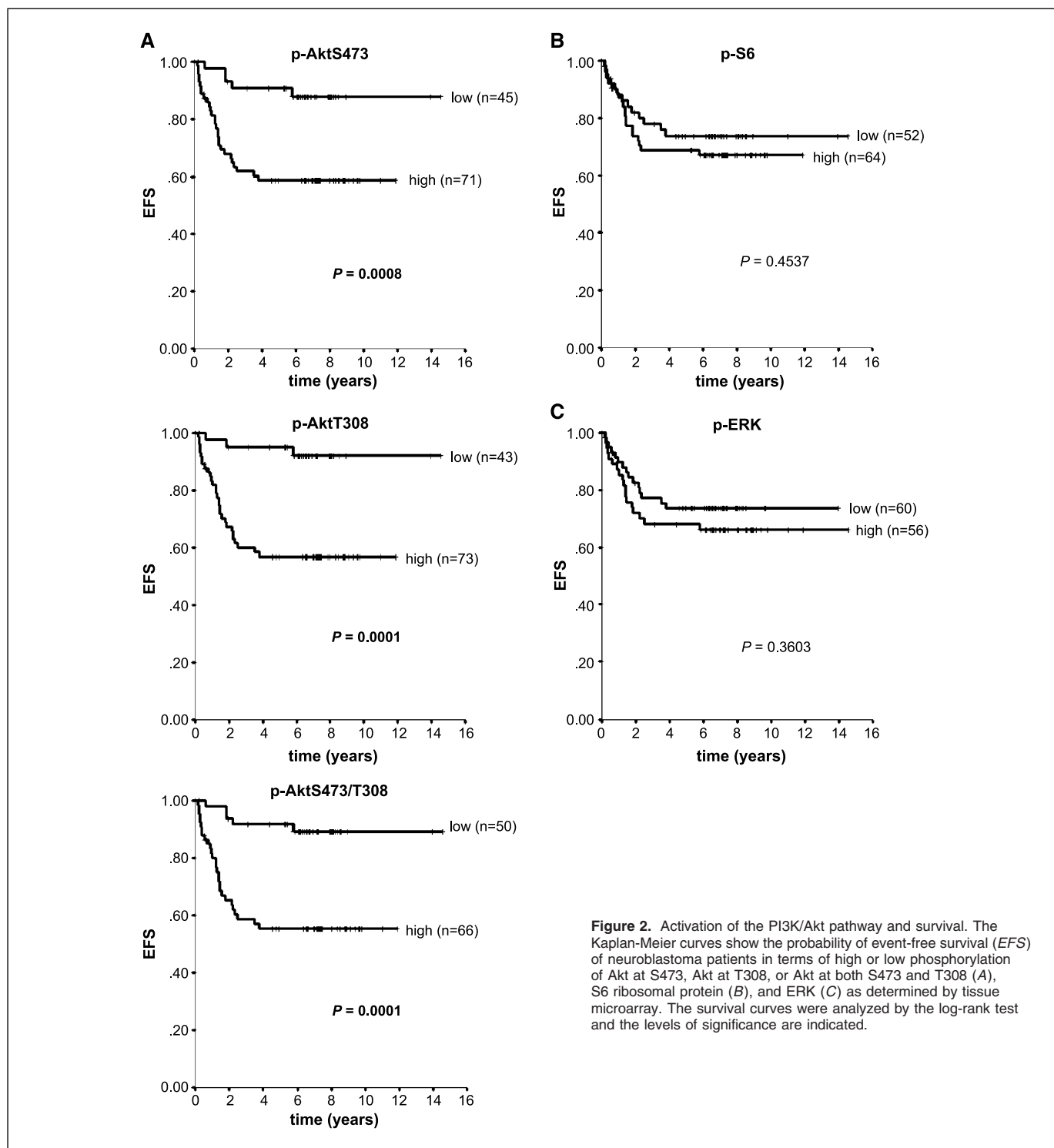

Figure 2. Activation of the PI3K/Akt pathway and survival. The Kaplan-Meier curves show the probability of event-free survival (*EFS*) of neuroblastoma patients in terms of high or low phosphorylation of Akt at S473, Akt at T308, or Akt at both S473 and T308 (*A*), S6 ribosomal protein (*B*), and ERK (*C*) as determined by tissue microarray. The survival curves were analyzed by the log-rank test and the levels of significance are indicated.

Table 2. Correlation of the phosphorylation status of Akt, S6 ribosomal protein, or ERK and survival in primary neuroblastoma

Phosphorylation	n	3-y EFS	3-y OS
p-AktS473			
Low	45	91 ± 4	98 ± 2
High	71	62 ± 6	84 ± 5
P (log-rank)		**0.0008**	**0.0156**
p-AktT308			
Low	43	95 ± 3	100
High	73	60 ± 6	83 ± 5
P (log-rank)		**0.0001**	**0.0017**
p-AktS473/T308			
Low	50	92 ± 4	98 ± 2
High	66	59 ± 6	82 ± 5
P (log-rank)		**0.0001**	**0.0039**
p-S6			
Low	52	78 ± 6	88 ± 5
High	64	69 ± 6	90 ± 4
P (log-rank)		0.4537	0.9070
p-ERK			
Low	60	77 ± 6	91 ± 4
High	56	68 ± 6	87 ± 5
P (log-rank)		0.3603	0.4317

NOTE: Phosphorylation of Akt at S473 (AktS473) or at T308 (AktT308), S6 ribosomal protein, and ERK was analyzed by immunohistochemistry on a tissue microarray. Survival curves were calculated according to Kaplan-Meier and compared with log-rank test. Three-year event-free survival (EFS) and overall survival (OS) for samples with low or high phosphorylation of Akt at S473 (AktS473), at T308 (AktT308), at both S473 and T308 (AktS473/T308), S6 ribosomal protein, and ERK are shown. Statistically significant correlations are indicated in bold.

experiments. Together, this set of experiments shows that no detectable activation of Akt occurs under complete serum starvation in neuroblastoma cell lines, whereas some activation of Akt is detected in the majority of neuroblastoma cell lines cultured in medium containing 10% FCS and strong activation of Akt occurs on stimulation with IGF-I.
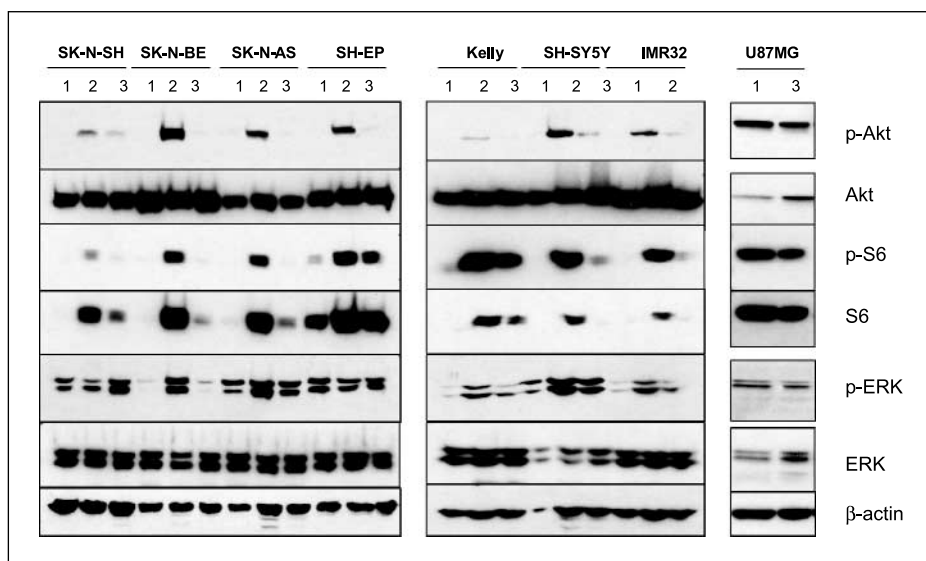
Activation of Akt rescues neuroblastoma cells from cytotoxic drug– or TRAIL-induced apoptosis. In light of our findings that activation of Akt correlates with poor prognosis in neuroblastoma, we wished to explore in more detail the role of the PI3K/Akt survival cascade in regulating apoptosis in neuroblastoma cells. To address this issue, we used IGF-I to stimulate Akt activation in prototype S-type (SH-EP) and N-type (SH-SY5Y) neuroblastoma cell lines. S-type (substrate adherent) and N-type (neuroblastic) cell lines are considered to correspond to distinct cell types present in human neuroblastoma tumors (25).

As shown in Fig. 4A, both SH-EP and SH-SY5Y neuroblastoma cells express IGF receptor on their cell surface. Stimulation with IGF-I resulted in rapid and prolonged phosphorylation of Akt (Fig. 4B). In addition, treatment with IGF-I rapidly triggered phosphorylation of S6 ribosomal protein (Fig. 4B). Compared with Akt, phosphorylation of S6 ribosomal protein was transient and declined after 24 h, and then became undetectable at 48 h (Fig. 4B). Because childhood tumors such as neuroblastoma have been reported to preferentially express IGF-II (26), we also compared activation of Akt by IGF-I and IGF-II. As shown in Fig. 4B, IGF-I and IGF-II similarly stimulated phosphorylation of Akt in SH-EP neuroblastoma cells. Because we observed no differences between IGF-I and IGF-II in their ability to activate Akt, we used IGF-I for further experiments.

Next, we investigated whether or not activation of Akt interferes with the ability of neuroblastoma cells to undergo apoptosis. To this end, SH-EP and SH-SY5Y neuroblastoma cells were left untreated or were pretreated with IGF-I for 4 h to stimulate Akt before apoptosis was induced in the presence or absence of IGF-I. Importantly, activation of Akt by pretreatment with IGF-I significantly reduced doxorubicin-induced apoptosis in both SH-EP and SH-SY5Y neuroblastoma cells in a dose- and time-dependent manner (Fig. 4C). Similarly, activation of Akt by pretreatment with IGF-I resulted in a significant decrease of cisplatin-induced apoptosis in SH-EP and SH-SY5Y neuroblastoma cells (Fig. 4C).

To examine whether or not apoptosis resistance mediated by Akt was restricted to cytotoxic drugs, which predominately activate

Figure 3. Activation of the PI3K/Akt pathway in neuroblastoma cell lines. SK-N-SH, SK-N-BE, SK-N-AS, SH-EP, Kelly, SH-SY5Y, and IMR32 neuroblastoma cells were cultured for 24 h in medium containing 0% FCS (*1*), were stimulated for 1 h with 200 ng/mL IGF-I in medium containing 0% FCS (*2*), or were cultured for 24 h in medium containing 10% FCS (*3*). U87MG glioblastoma cells cultured for 24 h in medium containing 0% FCS (*1*) or 10% FCS (*3*) were used as a positive control for phosphorylation of Akt, S6 ribosomal protein, and ERK. Protein levels of phospho-AktS473, Akt, phospho-S6 ribosomal protein, S6 ribosomal protein, phospho-ERK, ERK, and β-actin were assessed by Western blot analysis.
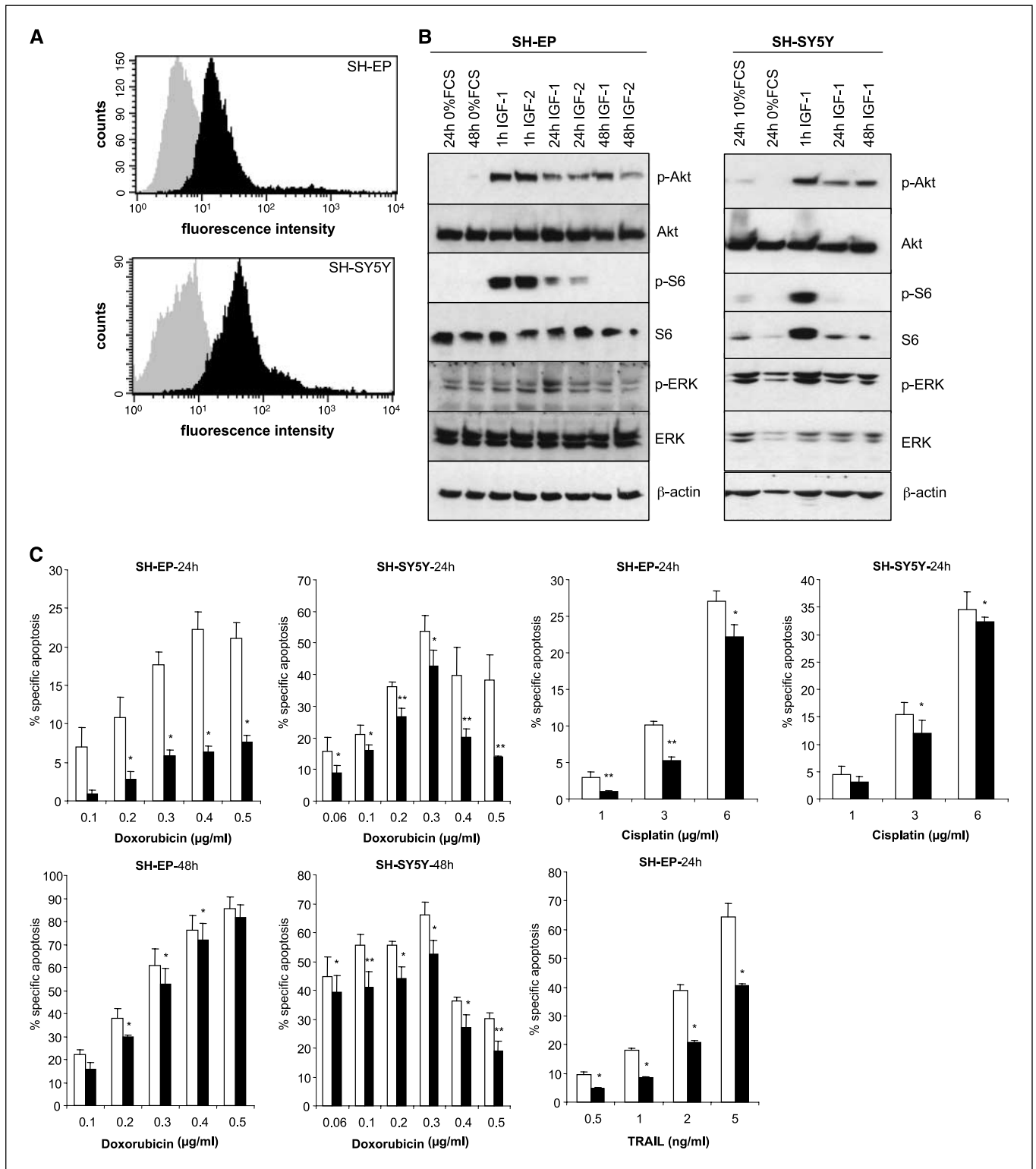
Figure 4. Activation of Akt rescues neuroblastoma cells from cytotoxic drug– or TRAIL-induced apoptosis. *A,* IGF-I receptor expression in neuroblastoma cell lines. Surface expression of IGF-I receptor on SH-EP and SH-SY5Y neuroblastoma cells was determined by FACS analysis using IGF-I receptor antibody (*black*) or isotype control (*gray*). *B,* effect of IGF-I and IGF-II on phosphorylation of Akt, S6 ribosomal protein, and ERK. SH-EP or SH-SY5Y neuroblastoma cells were cultured in medium containing 0% or 10% FCS or were stimulated with 200 ng/mL IGF-I or IGF-II in medium containing 0% FCS for indicated time points. Protein levels of phospho-AktS473, Akt, phospho-S6 ribosomal protein, S6 ribosomal protein, phospho-ERK, ERK, and β-actin were assessed by Western blot. *C,* effect of IGF-I on cytotoxic drug– or TRAIL-induced apoptosis. SH-EP or SH-SY5Y neuroblastoma cells were pretreated or not with 200 ng/mL IGF-I for 4 h and then treated with doxorubicin, cisplatin, or TRAIL in the absence (□) or presence (■) of 200 ng/mL IGF-I for indicated times and concentrations. Apoptosis was measured by FACS analysis of DNA fragmentation of propidium iodide–stained nuclei; percentage of specific apoptosis is shown. *Columns,* mean of three independent experiments done in duplicates or triplicates; *bars,* SE. Apoptosis in the presence of IGF-I alone was <5%. *, $P < 0.05$; **, $P < 0.001$, treatment with IGF-I versus treatment without IGF-I (Student's *t* test).

the intrinsic pathway of apoptosis, we then extended our studies to the extrinsic pathway using the death receptor ligand TRAIL. In addition, activation of Akt by IGF-I significantly reduced TRAIL-induced apoptosis in SH-EP cells (Fig. 4*C*). TRAIL could not be assessed in SH-SY5Y cells because they lack expression of caspase-8, which is an essential component of the apoptotic signal transduction pathway triggered by TRAIL (27). Together, these findings show that activation of Akt by IGF-I reduces anticancer drug– or TRAIL-induced apoptosis in both S- and N-type neuroblastoma cells.

Inhibition of PI3K/Akt abolishes IGF-I–mediated protection against doxorubicin- or TRAIL-induced apoptosis. IGF-I has been reported to mediate survival via the PI3K/Akt and/or Raf/MEK/ERK pathway (28). Therefore, to further elucidate the specific contribution of PI3K/Akt to IGF-I–mediated apoptosis resistance, we used LY294002, a competitive and reversible inhibitor of the ATP-binding site of PI3K (29). To analyze whether or not inhibition of PI3K by LY294002 was effective in neuroblastoma cells, we determined phosphorylation of Akt, a downstream target of PI3K, by Western blot analysis. As shown in Fig. 5*A* and *B*, LY294002 strongly inhibited phosphorylation of Akt in response to stimulation with IGF-I in a concentration-dependent manner. Next, we investigated the ability of IGF-I to protect neuroblastoma cells against doxorubicin- or TRAIL-induced apoptosis in the presence or absence of the PI3K inhibitor LY294002. Importantly, inhibition of PI3K by LY294002 completely reversed the IGF-I–mediated protection against doxorubicin- or TRAIL-induced apoptosis (Fig. 5*C* and *D*). This shows that IGF-I confers resistance towards doxorubicin- or TRAIL-induced apoptosis in a PI3K-dependent manner in neuroblastoma cells.

Discussion

Despite intensive, multimodality therapy, the cure rate of advanced neuroblastoma has only modestly improved in recent years (1). Therefore, a better understanding of the pathways responsible for neuroblastoma progression and treatment resistance may lead to the development of more effective, less toxic therapies (4). The PI3K/Akt pathway is a key mediator of cell survival signals, and human malignancies with high active Akt levels have been reported to be resistant to various treatments (5, 18). Whereas deregulated signaling via the PI3K/Akt pathway has been associated with poor prognosis in several human cancers (5), the question whether or not the activation status of key components of this survival cascade bears prognostic effect on outcome in neuroblastoma has not previously been addressed.

Here, we provide for the first time evidence that phosphorylation of Akt at S473 and/or T308, S6 ribosomal protein, and ERK is a frequent event in neuroblastoma. Moreover, we identified Akt activation as a novel prognostic indicator of reduced event-free or overall survival in neuroblastoma. In addition, Akt activation correlated with established variables of aggressive disease, including *MYCN* amplification, 1p36 aberrations, advanced disease stage, age at diagnosis, and unfavorable histology. Monitoring Akt at T308 or both phosphorylation sites compared with S473 phosphorylation improved the assessment of Akt activation in neuroblastoma samples. In contrast to Akt, phosphorylation of S6 ribosomal protein or ERK did not correlate with survival or variables of advanced disease in neuroblastoma. The findings in primary neuroblastoma samples were corroborated by parallel

experiments in neuroblastoma cell lines showing that activation of Akt by IGF-I protected neuroblastoma cells from TRAIL- or chemotherapy-induced apoptosis in a PI3K-dependent manner. Together, these data suggest that Akt presents a clinically relevant target to enhance the efficacy of cytotoxic therapies in neuroblastoma.

Aberrant activation of Akt has previously been linked to poor prognosis in other human malignancies (e.g., glioblastoma and breast carcinoma; refs. 6, 7). Our study is the first to report a correlation between the activation status of Akt and reduced survival in neuroblastoma. Thus, it extends the clinical relevance of Akt to the most common extracranial solid tumor of childhood. Assessment of Akt activation by monitoring phosphorylation at T308 or at both T308 and S473 improved the prognostic significance of Akt activation in neuroblastoma specimens compared with determining only S473 phosphorylation. Similarly, evaluation of both Akt phosphorylation sites has recently been reported to improve the assessment of Akt activation in non–small-cell lung cancer (30). This may reflect that phosphorylation of both sites is required for full activation of Akt (5). Accordingly, S473 phosphorylation does not necessarily correlate with Akt activity (e.g., in PDK-1-deficient cells that lack T308 phosphorylation on IGF-I stimulation; ref. 31). Thus, evaluation of both T308 and S473 phosphorylation may be a better surrogate for Akt activity in clinical specimens. Our finding that Akt activation correlated with several variables of aggressive disease in neuroblastoma, including *MYCN* amplification, 1p36 aberrations, advanced disease stage, age at diagnosis, and unfavorable histology, may reflect its association with poor prognosis. Alternatively, correlation of phosphorylated Akt with *MYCN* amplification and 1p36 aberrations may point to a novel link between Akt and genetic aberrations in neuroblastoma because activation of Akt has recently been reported to contribute to genomic instability of tumor cells (32, 33). However, whether or not such a link between Akt and genomic instability exists in neuroblastoma is subject to future investigations. Because only phosphorylation of Akt, but not of ERK or S6 ribosomal protein, was prognostically significant, although there was a correlation among the three phospho-proteins analyzed, these findings suggest that these proteins may primarily control distinct pathways with differential prognostic effects (e.g., metabolism, differentiation, cell death, and survival).

The PI3K/Akt pathway can be up-regulated in human cancers through several mechanisms. Perhaps the most commonly known mechanisms comprise mutations or deletions of key components of the signaling cascade (e.g., *PTEN* or *PIK3CA*) or through amplification or overexpression of critical growth factor receptors (9, 10, 34). The cause of Akt activation in neuroblastoma may involve deregulated growth factor signaling (e.g., triggered by the IGF system in a paracrine or autocrine manner; ref. 11). In support of this notion, we found strong phosphorylation of Akt in neuroblastoma cells stimulated with IGF-I or IGF-II in line with other reports (35, 36). As neuroblastoma is a tumor of the neural crest, neurotrophins and their receptors (e.g., nerve growth factor/TrkA and BDNF/TrkB) are also likely involved in regulating Akt activation *in vivo* (1). BDNF/TrkB stimulation has been reported to activate the PI3K/Akt pathway in neuroblastoma cells (37–39). It will be subject to future studies to explore activators of Akt in neuroblastoma *in vivo* (e.g., by correlating Akt phosphorylation with expression of TrkA, TrkB, or IGF receptors and their corresponding ligands). Deletions of the tumor suppressor gene *PTEN*, an
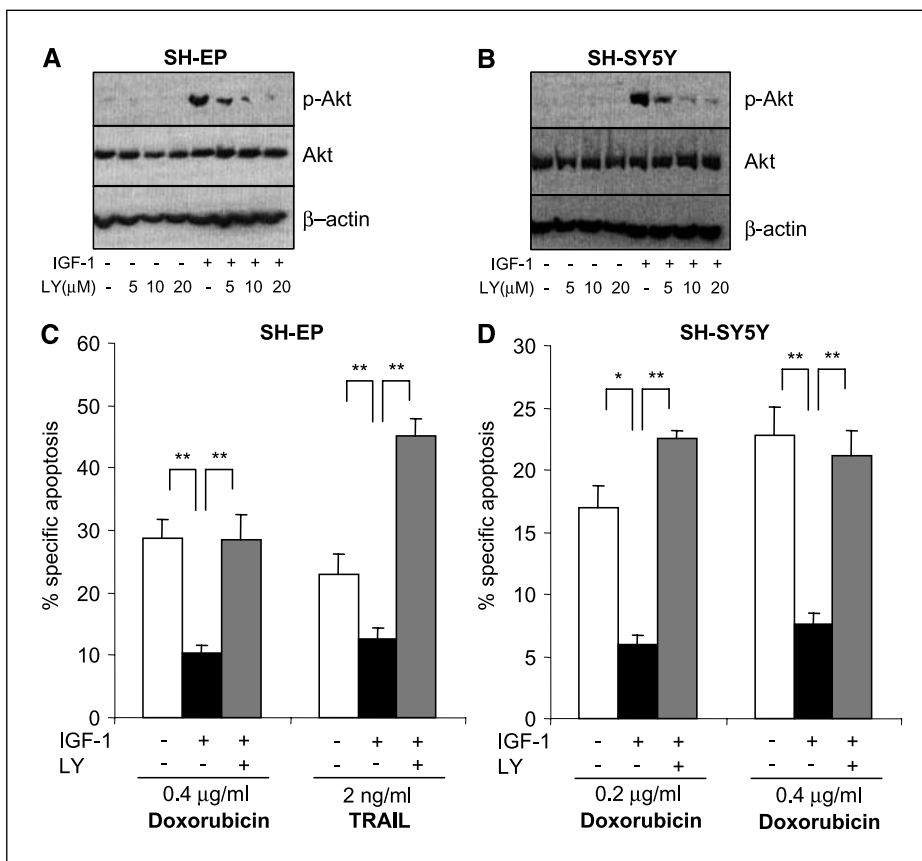
Figure 5. Inhibition of PI3K/Akt abolishes IGF-I–mediated protection against doxorubicin- or TRAIL-induced apoptosis. *A* and *B,* effect of PI3K inhibition on IGF-I–mediated phosphorylation of Akt. SH-EP (*A*) and SH-SY5Y (*B*) neuroblastoma cells were cultured for 24 h in the absence (−) or presence (+) of 200 ng/mL IGF-I and/or indicated concentrations of the PI3K inhibitor LY294002. Protein levels of phospho-AktS473, Akt, and β-actin were assessed by Western blot. *C* and *D,* effect of PI3K inhibition on IGF-I–mediated protection against doxorubicin- or TRAIL-induced apoptosis. SH-EP (*C*) or SH-SY5Y (*D*) neuroblastoma cells were pretreated or not with 200 ng/mL IGF-I for 4 h and then treated for 24 h with doxorubicin or TRAIL in the absence (□) or presence (■) of 200 ng/mL IGF-I, or with 200 ng/mL IGF-I and 20 μmol/L LY294002 (▨). Apoptosis was measured by FACS analysis of DNA fragmentation of propidium iodide–stained nuclei; percentage of specific apoptosis is shown. *Columns,* mean of three independent experiments done in triplicate; *bars,* SE. Apoptosis in the presence of IGF-I or LY294002 alone was <5% or 10%, respectively. *, $P < 0.05$; **, $P < 0.001$ (Student's *t* test).

antagonists of PI3K signaling, are rare in neuroblastoma (40), whereas *PTEN* mutations are a frequent cause of aberrant activation of PI3K/Akt in glioblastoma (41). Collectively, these findings support a model where activation of Akt in neuroblastoma may predominantly be caused by elevated signaling through growth factor receptors, promoting growth and conferring resistance to cell death.

Our findings that activation of Akt by IGF-I protected neuroblastoma cells against TRAIL- or cytotoxic drug–induced apoptosis are in line with mounting evidence that activation of this survival cascade can rescue neuroblastoma cells from cell death (e.g., in response to anticancer agents). To this end, aberrant stimulation of the BDNF/TrkB pathway was reported to enhance resistance of neuroblastoma cells to chemotherapy in a PI3K-dependent manner (37, 39). Using pharmacologic and genetic tools, Akt was recently identified as a key component of the BDNF/TrkB–mediated survival signaling and chemoresistance in neuroblastoma cells (38). Previously, IGF-I has been reported to rescue neuroblastoma cells from hyperosmotic stress–, peroxynitrite-, hypoxia-, doxorubicin-, or TNFα-induced apoptosis (36, 42–45). Our study extends these findings by showing that IGF-I also protects neuroblastoma cells from apoptosis induced by the death-inducing ligand TRAIL. Together, these data indicate that activation of Akt by IGF-I confers resistance to neuroblastoma cells against a variety of cytotoxic stimuli. Because there is accumulating evidence that TRAIL may play an important role as effector molecule of the innate immune response in tumor surveillance (46), protection from TRAIL-induced apoptosis by

activation of Akt may promote progression of neuroblastoma. In addition, recombinant soluble TRAIL and agonistic TRAIL receptor antibodies are currently evaluated in early clinical trials for the treatment of cancer. Thus, strategies to enhance the efficacy of TRAIL-based therapies (e.g., small-molecule PI3K inhibitors) are particularly interesting for molecular targeted cancer therapy in neuroblastoma.

By showing that high phosphorylation of Akt *in vivo* correlates with reduced survival of neuroblastoma patients and that activation of Akt protects neuroblastoma cells against TRAIL- or chemotherapy-induced apoptosis, our results indicate that Akt plays an important role in promoting survival in neuroblastoma. These findings have clinical implications for the development of experimental approaches in neuroblastoma therapy because resistance to undergo programmed cell death is a major cause of nonresponsiveness of cancers, such as neuroblastoma, leading to treatment failure. Thus, Akt represents a clinically relevant target (e.g., using small-molecule inhibitors) to enhance the efficacy of anticancer therapy and to attain therapeutic gain in the treatment of neuroblastoma.

Acknowledgments

References

1. Brodeur GM. Neuroblastoma: biological insights into a clinical enigma. Nat Rev Cancer 2003;3:203–16.
2. Berthold F, Hero B. Neuroblastoma: current drug therapy recommendations as part of the total treatment approach. Drugs 2000;59:1261–77.
3. Berthold F, Hero B, Kremens B, et al. Long-term results and risk profiles of patients in five consecutive trials (1979-1997) with stage 4 neuroblastoma over 1 year of age. Cancer Lett 2003;197:11–7.
4. Schwab M, Westermann F, Hero B, Berthold F. Neuroblastoma: biology and molecular and chromosomal pathology. Lancet Oncol 2003;4:472–80.
5. Vivanco I, Sawyers CL. The phosphatidylinositol 3-Kinase AKT pathway in human cancer. Nat Rev Cancer 2002;2:489–501.
6. Perez-Tenorio G, Stal O; Southeast Sweden Breast Cancer Group. Activation of AKT/PKB in breast cancer predicts a worse outcome among endocrine treated patients. Br J Cancer 2002;86:540–5.
7. Chakravarti A, Zhai G, Suzuki Y, et al. The prognostic significance of phosphatidylinositol 3-kinase pathway activation in human gliomas. J Clin Oncol 2004;22:1926–33.
8. Choe G, Horvath S, Cloughesy TF, et al. Analysis of the phosphatidylinositol 3′-kinase signaling pathway *in vivo* in glioblastoma patients. Cancer Res 2003;63:2742–6.
9. Cully M, You H, Levine AJ, Mak TW. Beyond PTEN mutations: the PI3K pathway as an integrator of multiple inputs during tumorigenesis. Nat Rev Cancer 2006;6:184–92.
10. Blume-Jensen P, Hunter T. Oncogenic kinase signalling. Nature 2001;411:355–65.
11. Zumkeller W, Schwab M. Insulin-like growth factor system in neuroblastoma tumorigenesis and apoptosis: potential diagnostic and therapeutic perspectives. Horm Metab Res 1999;31:138–41.
12. Hengartner MO. The biochemistry of apoptosis. Nature 2000;407:770–6.
13. Fulda S, Debatin KM. Targeting apoptosis pathways in cancer therapy. Curr Cancer Drug Targets 2004;4:569–76.
14. Fulda S, Debatin KM. Apoptosis pathways in neuroblastoma therapy. Cancer Lett 2003;197:131–5.
15. Lowe SW, Cepero E, Evan G. Intrinsic tumour suppression. Nature 2004;432:307–15.
16. Ashkenazi A. Targeting death and decoy receptors of the tumour-necrosis factor superfamily. Nat Rev Cancer 2002;2:420–30.
17. Saelens X, Festjens N, Vande Walle L, van Gurp M, van Loo G, Vandenabeele P. Toxic proteins released from mitochondria in cell death. Oncogene 2004;23:2861–74.
18. West KA, Castillo SS, Dennis PA. Activation of the PI3K/Akt pathway and chemotherapeutic resistance. Drug Resist Update 2002;5:234–48.

19. Workman P. Inhibiting the phosphoinositide 3-kinase pathway for cancer treatment. Biochem Soc Trans 2004;32:393–6.
20. Ambros PF, Ambros IM; SIOP Europe Neuroblastoma Pathology, Biology and Bone Marrow Group. Pathology and biology guidelines for resectable and unresectable neuroblastic tumors and bone marrow examination guidelines. Med Pediatr Oncol 2001;37:492–504.
21. Fulda S, Sieverts H, Friesen C, Herr I, Debatin KM. The CD95 (APO-1/Fas) system mediates drug-induced apoptosis in neuroblastoma cells. Cancer Res 1997;57:823–9.
22. Scheid MP, Woodgett JR. Protein kinases: six degrees of separation? Curr Biol 2000;10:R191–4.
23. Rommel C, Clarke BA, Zimmermann S, et al. Differentiation stage-specific inhibition of the Raf-MEK-ERK Pathway by Akt. Science 1999;286:1738–41.
24. Zimmermann S, Moelling K. Phosphorylation and regulation of Raf by Akt (protein kinase B). Science 1999;286:1741–4.
25. Ross RA, Biedler JL, Spengler BA. A role for distinct cell types in determining malignancy in human neuroblastoma cell lines and tumors. Cancer Lett 2003;197:35–9.
26. Cianfarani S, Rossi P. Neuroblastoma and insulin-like growth factor system. New insights and clinical perspectives. Eur J Pediatr 1997;156:256–61.
27. Fulda S, Kufer MU, Meyer E, van Valen F, Dockhorn-Dworniczak B, Debatin KM. Sensitization for death receptor- or drug-induced apoptosis by re-expression of caspase-8 through demethylation or gene transfer. Oncogene 2001;20:5865–77.
28. Kurihara S, Hakuno F, Takahashi S. Insulin-like growth factor-I-dependent signal transduction pathways leading to the induction of cell growth and differentiation of human neuroblastoma cell line SH-SY5Y: the roles of MAP kinase pathway and PI 3-kinase pathway. Endocr J 2000;47:739–51.
29. Djordjevic S, Driscoll PC. Structural insight into substrate specificity and regulatory mechanisms of phosphoinositide 3-kinases. Trends Biochem Sci 2002;27:426–32.
30. Tsurutani J, Fukuoka J, Tsurutani H, et al. Evaluation of two phosphorylation sites improves the prognostic significance of Akt activation in non-small-cell lung cancer tumors. J Clin Oncol 2006;24:306–14.
31. Williams MR, Arthur JS, Balendran A, et al. The role of 3-phosphoinositide-dependent protein kinase 1 in activating AGC kinases defined in embryonic stem cells. Curr Biol 2000;10:439–48.
32. Jin J, Woodgett JR. Chronic activation of protein kinase Bbeta/Akt2 leads to multinucleation and cell fusion in human epithelial kidney cells: events associated with tumorigenesis. Oncogene 2005;24:5459–70.

33. Puc J, Keniry M, Li HS, et al. Lack of PTEN sequesters CHK1 and initiates genetic instability. Cancer Cell 2005;7:193–204.
34. Samuels Y, Wang Z, Bardelli A, et al. High frequency of mutations of the PIK3CA gene in human cancers. Science 2004;304:554.
35. Kim B, van Golen CM, Feldman EL. Insulin-like growth factor-I signaling in human neuroblastoma cells. Oncogene 2004;23:130–41.
36. van Golen CM, Schwab TS, Ignatoski KM, Ethier SP, Feldman EL. PTEN/MMAC1 overexpression decreases insulin-like growth factor-I-mediated protection from apoptosis in neuroblastoma cells. Cell Growth Differ 2001;12:371–8.
37. Jaboin J, Kim CJ, Kaplan DR, Thiele CJ. Brain-derived neurotrophic factor activation of TrkB protects neuroblastoma cells from chemotherapy-induced apoptosis via phosphatidylinositol 3′-kinase pathway. Cancer Res 2002;62:6756–63.
38. Li Z, Jaboin J, Dennis PA, Thiele CJ. Genetic and pharmacologic identification of Akt as a mediator of brain-derived neurotrophic factor/TrkB rescue of neuroblastoma cells from chemotherapy-induced cell death. Cancer Res 2005;65:2070–5.
39. Ho R, Eggert A, Hishiki T, et al. Resistance to chemotherapy mediated by TrkB in neuroblastomas. Cancer Res 2002;62:6462–6.
40. Munoz J, Lazcoz P, Inda MM, et al. Homozygous deletion and expression of PTEN and DMBT1 in human primary neuroblastoma and cell lines. Int J Cancer 2004;109:673–9.
41. Maher EA, Furnari FB, Bachoo RM, et al. Malignant glioma: genetics and biology of a grave matter. Genes Dev 2001;15:1311–33.
42. Liu XH, Yu EZ, Li YY, Rollwagen FM, Kagan E. RNA interference targeting Akt promotes apoptosis in hypoxia-exposed human neuroblastoma cells. Brain Res 2006;1070:24–30.
43. Gil-Ad I, Shtaif B, Luria D, Karp L, Fridman Y, Weizman A. Insulin-like-growth-factor-I (IGF-I) antagonizes apoptosis induced by serum deficiency and doxorubicin in neuronal cell culture. Growth Horm IGF Res 1999;9:458–64.
44. Kenchappa P. Rescue of TNFα-inhibited neuronal cells by IGF-1 involves Akt and c-Jun N-terminal kinases. J Neurosci Res 2004;76:466–74.
45. Saeki M, Maeda S, Wada K, Kamisaki Y. Insulin-like growth factor-1 protects peroxynitrite-induced cell death by preventing cytochrome *c*-induced caspase-3 activation. J Cell Biochem 2002;84:708–16.
46. Smyth MJ, Takeda K, Hayakawa Y, et al. Nature's TRAIL—on a path to cancer immunotherapy. Immunity 2003;18:1–6.